

Intrinsic brightness of SDSS objects is similar at all redshifts in de Sitter space

John B. Miller

Western Michigan University, Kalamazoo, MI 49008, USA

`john.b.miller@wmich.edu`

Thomas E. Miller

108 Titleist Drive, Bluefield, VA 24605, USA

`tommy81@alumni.princeton.edu`

ABSTRACT

The redshift-luminosity distributions for well-defined galaxies and quasars in the Sloan Digital Sky Survey (SDSS) are compared for the two redshift-distance relations of a Hubble redshift and a de Sitter redshift. Assuming a Hubble redshift, SDSS data can be interpreted as luminosity evolution following the Big Bang. In contrast, given a de Sitter redshift, the intrinsic brightness of objects at all redshifts is roughly the same. In a de Sitter universe, 95 per cent of SDSS galaxies and quasars fall into a magnitude range of only 2.8, and 99.7 per cent are within 5.4 mag. The comparable Hubble luminosity ranges are much larger: 95 per cent within 6.9, and 99.7 per cent within 11.5 mag. De Sitter space is now widely discussed, but the de Sitter redshift is hardly mentioned.

Subject headings: astronomical data bases: surveys – galaxies: distances and redshifts – cosmology: observations – cosmology: theory – physical data and processes: relativity – general: history and philosophy of astronomy

1. Introduction

Of late there has been an increase in the number of papers dealing with de Sitter space. The Maldacena conjecture or anti-de-Sitter space/conformal field theory (AdS/CFT) correspondence and the holographic principle have attracted interest (Maldacena 1998; Witten 1998; Metsaev & Tseytlin 1998; Gubser, Klebanov & Polyakov 1998), and there are earlier

examples (Chernikov & Tagirov 1968; Dyson 1972; Aldrovandi & Pereira 1996). However, there has been little discussion of the feature of de Sitter theory that was of most interest during its heyday in the 1920s: the de Sitter redshift.

Part of the reason for this is that the Hubble redshift has been extensively studied and is widely accepted. Supernovae studies have recently provided data consistent with the Hubble redshift. The de Sitter redshift was abandoned by its own author (de Sitter 1930) in favor of the time-dependent solution of Lemaître (1931). With few exceptions (Hawkins 1960; Miller & Miller 1995), the de Sitter redshift has not been seriously reconsidered.

However, it may be possible that the world is actually, not merely asymptotically, of a de Sitter nature. We reconsider the de Sitter redshift in its original astronomical context.

2. De Sitter Geometry

Much of the following is adapted from the original paper by de Sitter (1917). We retain de Sitter’s original notation as much as possible, even though this notation may sometimes conflict with modern conventions. We adopt these definitions:

- $\theta, \psi, \omega, \zeta, \chi \equiv$ angular coordinates,
- $x, y, z, u \equiv$ Euclidean coordinates,
- $t, \tilde{t} \equiv$ time coordinates,
- $r_1 \equiv$ radial pseudo-Euclidean coordinate,
- $r \equiv$ radial elliptical coordinate,
- $h \equiv$ radial hyperbolic coordinate,
- $R \equiv$ radius of curvature,
- $\lambda \equiv$ cosmological constant,
- $\rho \equiv$ mass density,
- $\kappa \equiv$ gravitational constant.

In two-dimensional, negatively-curved spacetime, the line element is

$$ds^2 = -R^2 (d\psi^2 + \sin^2 \psi d\theta^2).$$

The three-dimensional version is

$$ds^2 = -R^2 [d\zeta^2 + \sin^2 \zeta (d\psi^2 + \sin^2 \psi d\theta^2)].$$

The four-dimensional version is

$$ds^2 = -R^2 \{d\omega^2 + \sin^2 \omega [d\zeta^2 + \sin^2 \zeta (d\psi^2 + \sin^2 \psi d\theta^2)]\}. \quad (1)$$

This satisfies Einsteins gravitational field equations

$$G_{\mu\nu} - \lambda g_{\mu\nu} = -\kappa T_{\mu\nu} + \frac{1}{2}g_{\mu\nu}T$$

with

$$R^2 = \frac{3}{\lambda} = \frac{3c^2}{8\pi\kappa\rho}.$$

In order to avoid imaginary angles, we can substitute

$$\begin{aligned} \omega &= i\omega', \\ \zeta &= i\zeta'. \end{aligned}$$

Then the line-element becomes

$$ds^2 = R^2 \{d\omega'^2 - \sinh^2 \omega' [d\zeta'^2 + \sinh^2 \zeta' (d\psi^2 + \sin^2 \psi d\theta^2)]\}. \quad (2)$$

Transforming to pseudo-Euclidean coordinates

$$\begin{aligned} r_1 &= R \sinh \omega' \sinh \zeta', & \tilde{t} &= R \sinh \omega' \cosh \zeta', \\ x &= r_1 \sin \psi \sin \theta, \\ y &= r_1 \sin \psi \cos \theta, & u &= R \cosh \omega', \\ z &= r_1 \cos \psi, \end{aligned}$$

we have

$$ds^2 = -dx^2 - dy^2 - dz^2 + d\tilde{t}^2 - du^2 \quad (3)$$

and

$$R^2 - x^2 - y^2 - z^2 + \tilde{t}^2 - u^2 = 0.$$

Then by the transformation

$$\begin{aligned} z_1 &= ix, \\ z_2 &= iy, \\ z_3 &= iz, \\ z_4 &= \tilde{t}, \\ z_5 &= iu, \end{aligned}$$

we obtain the result

$$ds^2 = dz_1^2 + dz_2^2 + dz_3^2 + dz_4^2 + dz_5^2, \quad (4)$$

where

$$z_1^2 + z_2^2 + z_3^2 + z_4^2 + z_5^2 = (iR)^2. \quad (5)$$

The de Sitter metrics given by equations (1), (2), (3), and (4) demonstrate that in de Sitter spacetime, there is no preferred origin in either space or time, but with these metrics, time and space are mingled so that conventional rulers and clocks are not useful.

[Equation (5) is] the equation which determines that four-dimensional surface in the five-dimensional manifold that corresponds to space-time. In accordance with this result we can regard the geometry of the de Sitter universe as that holding on the surface of a sphere embedded in five-dimensional Euclidean space. And, as in the case of the Einstein universe, we gain an added intuitional appreciation of the homogeneity of the de Sitter model. It may be emphasized, nevertheless, that the formal simplicity in the expression for the line element given by [equation (5)] is achieved at the expense of losing track of the physical distinction between space-like intervals which are to be measured in principle by the use of metre sticks and time-like intervals which are measurable with the help of clocks. (Tolman 1934)

Static de Sitter metrics for which the $g_{\mu\nu}$ are independent of the time coordinate are of more physical interest.

In both systems A [Einstein] and B [de Sitter] it is always possible, at every point of the four-dimensional time-space, to find systems of reference in which the $g_{\mu\nu}$ depend only on one space-variable (the “radius-vector”), and not on the “time.” In the system A the “time” of these systems of reference is the same always and everywhere, in B it is not. In B there is no universal time; there is no essential difference between the “time” and the other three coordinates. None of them has any real physical meaning. (de Sitter 1917)

To obtain a more traditional de Sitter line element, we transform coordinates

$$\begin{aligned} \tilde{t} &= \sqrt{R^2 - r_1^2} \sinh\left(\frac{t}{R}\right), \\ u &= \sqrt{R^2 - r_1^2} \cosh\left(\frac{t}{R}\right), \end{aligned}$$

yielding the well-known pseudo-Euclidean de Sitter metric corresponding to the inside of a sphere $r_1 \leq R$ in Euclidean space,

$$ds^2 = - \left(1 - \frac{r_1^2}{R^2}\right)^{-1} dr_1^2 - r_1^2 [d\psi^2 + \sin^2 \psi d\theta^2] + \left(1 - \frac{r_1^2}{R^2}\right) dt^2 \quad (6)$$

(choosing units so that $c = 1$). This is one of the most common forms of the static (time-independent) de Sitter metric. It is less symmetric, but in some ways more intuitive than equation (1) or equation (4). Time and space have been disentangled, imaginary coordinates have been rendered real, and the metric is time-independent: the $g_{\mu\nu}$ are a function of only the radial coordinate and not the time coordinate. The de Sitter metric given by equation (6) is unique in that the surface area increases with the square of the radial coordinate r_1 so that luminosity distance D_L is given simply by

$$D_L = r_1. \quad (7)$$

By the transformation

$$r_1 = R \sin \frac{r}{R},$$

we obtain the metric of elliptical space

$$ds^2 = -dr^2 - R^2 \sin^2 \frac{r}{R} [d\psi^2 + \sin^2 \psi d\theta^2] + \cos^2 \frac{r}{R} dt^2,$$

written more clearly by substituting an angular coordinate

$$r = R\chi,$$

so that

$$ds^2 = -R^2 d\chi^2 - R^2 \sin^2 \chi [d\psi^2 + \sin^2 \psi d\theta^2] + \cos^2 \chi dt^2. \quad (8)$$

This elliptical de Sitter metric suggests an interesting topology for de Sitter space, whereby antipodal points are identified, and the whole of space is mapped on to one-half of a one-sided hypersphere. This topological mapping can be intuitively represented in the two-dimensional case as the surface of a hemisphere in three-dimensional space with cross-connectivity.

For pseudo-Euclidean or elliptical de Sitter coordinates, the velocity of light is not constant. For example, given equation (8) the radial velocity of light $v = \cos \chi$. If we introduce a new variable h by the condition

$$\frac{dr}{dh} = \cos \chi,$$

of which the integral is

$$\sinh \frac{h}{R} = \tan \frac{r}{R},$$

the velocity of light will be constant in all directions (de Sitter 1917). The line element becomes

$$ds^2 = \frac{-dh^2 - R^2 \sinh^2 \frac{h}{R} [d\psi^2 + \sin^2 \psi d\theta^2] + dt^2}{\cosh^2 \frac{h}{R}} \quad (9)$$

The three-dimensional space of this system of reference is the space with constant negative curvature: the space of Lobachevsky (1830) and Bolyai (1832). This coordinate system is most natural if one takes the essence of relativity to be the inability of an observer to measure a difference in the speed of light.

Unfortunately, for the case of negative curvature there is no intuitive, isometric mapping of a complete, negatively-curved, two-dimensional surface in three-dimensional Euclidean space (Hilbert 1901). Mapping a two-dimensional space with negative curvature on to a surface in three-dimensional Euclidean space allows some features of the geometry to become intuitive, but only at the expense of other features that become distorted.

The various de Sitter metrics are useful in different ways. The metric given by equation (1) demonstrates that all points in the geometry are equivalent. The pseudo-Euclidean metric given by equation (6) is unique in that the surface area increases with the square of the radial coordinate r_1 . The elliptical metric given by equation (8) has an interesting topology. And the hyperbolic metric given by equation (9) has the unique property that the speed of light is the same at all places in all directions.

Typical de Sitter $g_{\mu\nu}$ are given in Table 1. Note that for static de Sitter coordinates,

$$g_{22} = R^2 (g_{44} - 1),$$

and that

$$g_{44} = (z + 1)^{-2}.$$

The ratio of the observed flux F_A from an object at a distance A with redshift z_A , and the observed flux F_B from a similar object at a distance B with redshift z_B , is given by

$$\frac{F_A}{F_B} = \frac{g_{22}^B}{g_{22}^A} = \frac{1 - g_{44}^B}{1 - g_{44}^A} = \frac{1 - (z_B + 1)^{-2}}{1 - (z_A + 1)^{-2}}, \quad (10)$$

where $g_{\mu\nu}^A$ and $g_{\mu\nu}^B$ are the values of the $g_{\mu\nu}$ at the radial coordinate distances A and B respectively. Apparent magnitude is defined as

$$m_A - m_B = -2.5 \log \left(\frac{F_A}{F_B} \right) \quad (11)$$

where m_A and m_B are the apparent magnitudes of objects at distances A and B. In accord with the tensor character of equation (10), the relationship between magnitude and redshift does not depend on the choice of hyperbolic, elliptical, or pseudo-Euclidean coordinates: it is independent of the choice of coordinate transformations. The distance coordinate is effectively eliminated.

No matter which coordinate transformation is chosen, luminosity distance D_L is a function of g_{22} ,

$$D_L = (-g_{22})^{\frac{1}{2}}. \quad (12)$$

The coordinate r_1 is convenient in that $D_L = r_1$, but the same results will be obtained if the transformations leading to χ or h are applied consistently. The choice of coordinate systems is largely one of convenience: the relationship between the two observables (z and m) and the derived quantity ($M_{\text{de Sitter}}$) will not be affected by choice of coordinates.

Several de Sitter metrics have been given above. There are many other coordinate transformations, but the static de Sitter metric is well represented by equations (6), (8), and (9), corresponding to flat, positively-curved, and negatively-curved space respectively.

3. Redshift and luminosity

Large astronomical distances cannot be directly measured but are inferred from redshift according to some redshift-distance law. Since only apparent magnitudes are actually measured, discussions about distances in astronomy are really discussions about the derived absolute magnitudes.

Absolute magnitude M is related to apparent magnitude m and luminosity distance D_L (with D_L in Mpc) by

$$M = m - 5 \log D_L - 25 \quad (13)$$

Although there are many different ‘nontrivial’ redshifts (Reboul 1981), we focus on two: the Hubble redshift and the de Sitter redshift.

3.1. Hubble

Assuming a Hubble law, the luminosity distance D_L is related to redshift z by

$$D_L = \frac{c}{H_0 q_0^2} \left[1 - q_0 + q_0 z + (q_0 - 1) (2q_0 z + 1)^{\frac{1}{2}} \right], \quad (14)$$

where H_0 is the Hubble constant, and q_0 is the deceleration constant (Zombeck 1990). We neglect the K-correction and the correction for interstellar absorption, which are both small, focusing on a general comparison of the Hubble and de Sitter redshifts. Assuming $q_0 = 1$, equation (14) becomes

$$D_L = \frac{cz}{H_0}. \quad (15)$$

Inserting this into equation (13), we obtain

$$M_{\text{Hubble}} = m - 5 \log(z) + C_{\text{Hubble}} \quad (16)$$

where

$$C_{\text{Hubble}} = -5 \log \frac{c}{H_0} - 25 \quad (17)$$

with H_0 in $\text{km s}^{-1} \text{Mpc}^{-1}$.

Assuming $H_0 = 75$ and $H_0 = 50$, we have respectively, $C_{\text{Hubble}} = -43.0$ and $C_{\text{Hubble}} = -43.9$. A different value of H_0 would shift the data by a fixed amount but will not affect the slope. For example, a change from $H_0 = 75$ to $H_0 = 50$ would make all objects brighter by

$$5 \log(50/75) = -0.88 \text{ mag.}$$

3.2. De Sitter

Assuming photons are emitted at a constant rate in all directions from similar objects at different radial distances, the flux from an object at a given coordinate distance will be inversely proportional to the surface area of the space at that distance. In Euclidean space, this gives rise to the familiar inverse-square law dimming since surface area increases as the distance squared. However, in non-Euclidean space, surface area is not proportional to the square of the radius.

Using Table 1, the de Sitter line element may be written as

$$ds^2 = g_{11}dr^2 + g_{22} [d\psi^2 + \sin^2 \psi d\theta^2] + g_{44}c^2 dt^2 \quad (18)$$

so that surface area is proportional to g_{22} . Only the metric of equation (6) has inverse-square law dimming, as noted above [equation (7)]. The de Sitter redshift can be given by

$$z = (g_{44})^{-\frac{1}{2}} - 1 = \left(1 - \frac{r_1^2}{R^2}\right)^{-\frac{1}{2}} - 1, \quad (19)$$

or

$$r_1 = R [1 - (z + 1)^{-2}]^{\frac{1}{2}}, \quad (20)$$

so that

$$M_{\text{de Sitter}} = m - 2.5 \log[1 - (z + 1)^{-2}] + C_{\text{de Sitter}}, \quad (21)$$

with $C_{\text{de Sitter}} = -5 \log R - 25$. For example, assuming $R = 10^{10}$ light-years (or equivalently density $\rho = 1.8 \times 10^{-29}$ g cm⁻³), one obtains $C_{\text{de Sitter}} = -42.4$ mag.

A determination of the actual value of $C_{\text{de Sitter}}$ is equivalent to a determination of the value of R , akin to a measurement of H_0 , and beyond the current scope of this work. The actual value of $C_{\text{de Sitter}}$ is not essential to the analysis, since changing $C_{\text{de Sitter}}$ will displace all of the data by a fixed amount.

4. Observations

We extracted galaxies and quasars from the Sloan Digital Sky Survey (Abazajian et al. 2009) that have redshift confidence greater than 0.95. The raw data (apparent magnitude vs. log redshift) are shown in Fig. 1, and the Hubble [equation (16)] and de Sitter [equation (21)] absolute magnitude transformations are shown in Fig. 2 and Fig. 3, respectively. We have assumed $C_{\text{Hubble}} = -43.0$ and $C_{\text{de Sitter}} = -42.4$ mag. We show only the R magnitude, but similar results are obtained with any of the *UGRIZ* magnitudes. Likewise, the results are not sensitive to the choice of redshift confidence.

The upward slope of Fig. 1 shows that, for low-redshift objects, dimness increases with increasing redshift and suggests that redshift is a distance effect, not a local or intrinsic phenomenon.

Assuming a Hubble redshift (Fig. 2), high-redshift objects are intrinsically brighter than low-redshift objects. This trend is currently interpreted as luminosity evolution following the Big Bang.

However, it may be that the data can be interpreted in a different, yet self-consistent way. Note the narrow range and roughly horizontal configuration of Fig. 3. Given a de Sitter redshift, the intrinsic brightness of objects at all redshifts is practically the same.

Assuming a de Sitter redshift, 99.7% of SDSS objects at all redshifts span a range of only 5.4 mag, while assuming a Hubble redshift, the range is more than double at 11.5 mag (Table 2). This may be a coincidence, but the de Sitter redshift is especially interesting in light of recent work on de Sitter space in allied fields.

Table 1: De Sitter geometry.

Geometry	Pseudo-Euclidean	Elliptical	Hyperbolic
Metric	Eq. (6)	Eq. (8)	Eq. (9)
Coordinates	r_1, ψ, θ, t	χ, ψ, θ, t	h, ψ, θ, t
g_{11}	$-\left(1 - \frac{r_1^2}{R^2}\right)^{-1}$	$-R^2$	$-\text{sech}^2 \frac{h}{R}$
g_{22}	$-r_1^2$	$-R^2 \sin^2 \chi$	$-R^2 \tanh^2 \frac{h}{R}$
g_{44}	$\left(1 - \frac{r_1^2}{R^2}\right)$	$\cos^2 \chi$	$\text{sech}^2 \frac{h}{R}$
$\frac{g_{22}}{R^2(g_{44}-1)}$	1	1	1

Table 2: SDSS absolute magnitude range.

Percentile	Hubble	De Sitter
$\Delta 68\%$	2.2	1.3
$\Delta 95\%$	6.9	2.8
$\Delta 99.7\%$	11.5	5.4

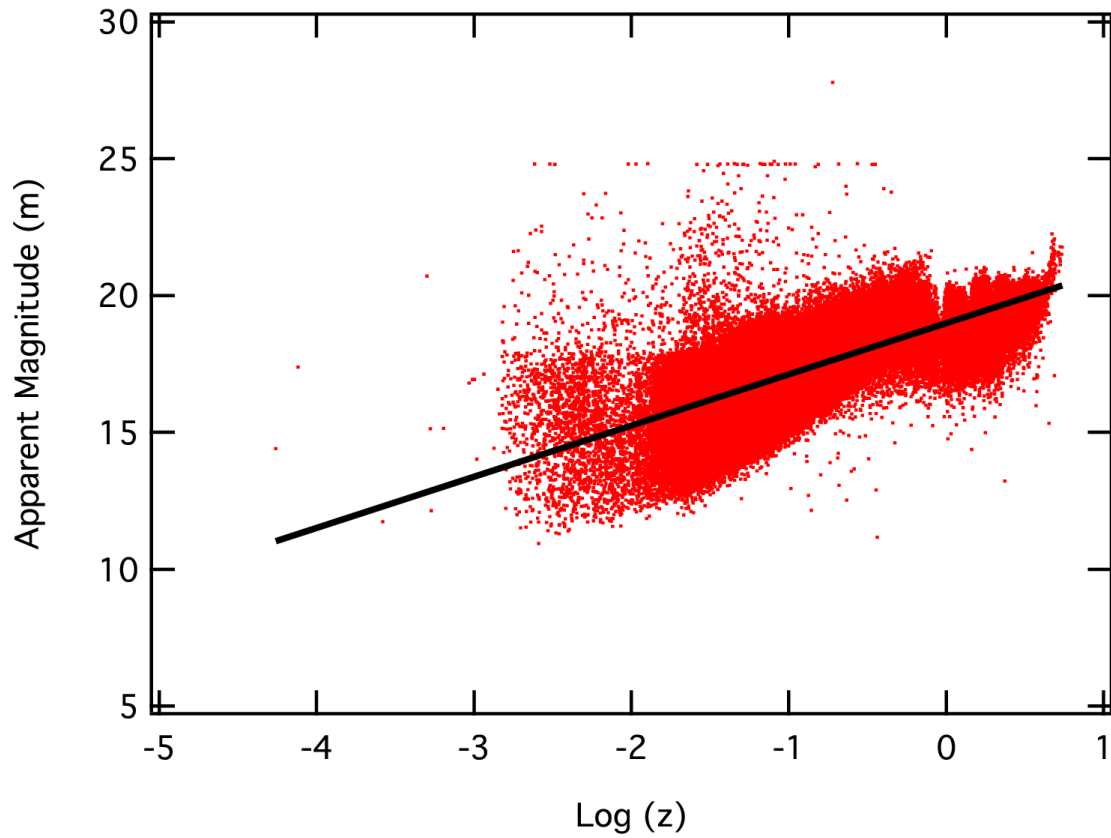


Fig. 1.— R -band magnitudes of 786409 SDSS DR7 objects with redshift confidence greater than 0.95 are plotted versus $\log(z)$. Of these, 717036 are galaxies, and 69373 are quasars. The line is a best fit to the data to show the general trend in the dataset.

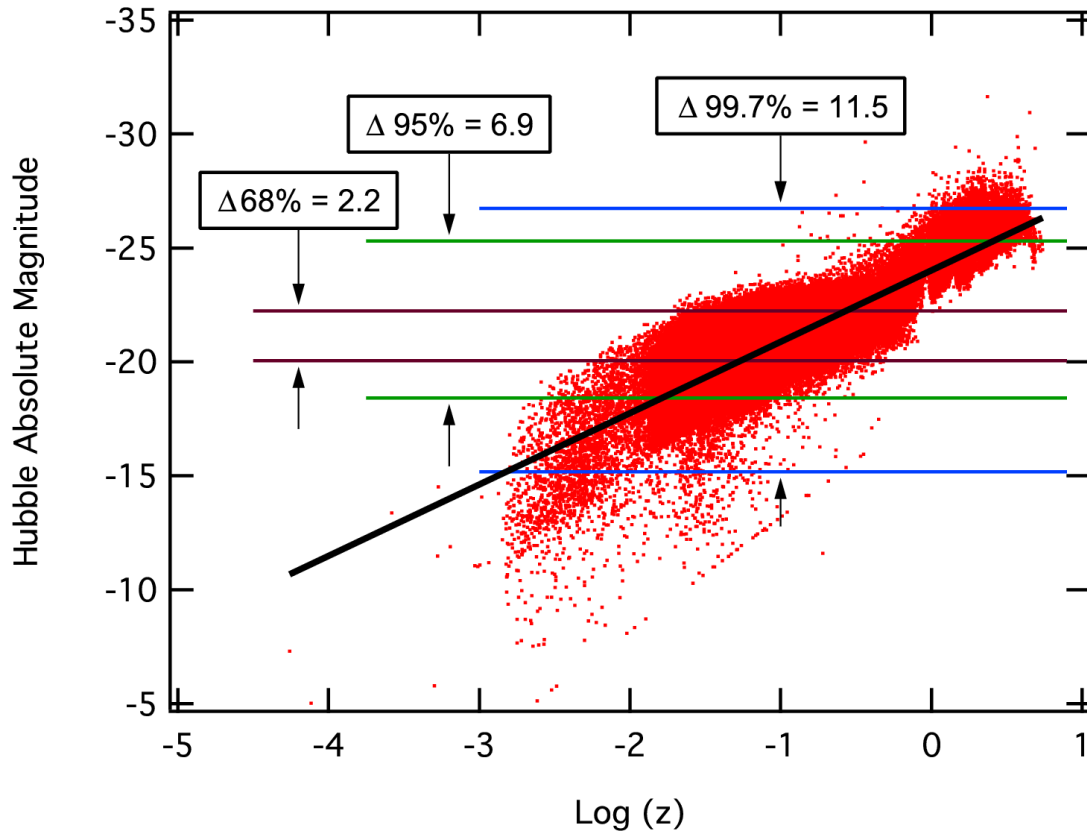


Fig. 2.— Hubble absolute magnitude versus $\log(z)$ for SDSS galaxies and quasars. There is increasing intrinsic brightness with increasing redshift, consistent with luminosity evolution in a Big Bang universe.

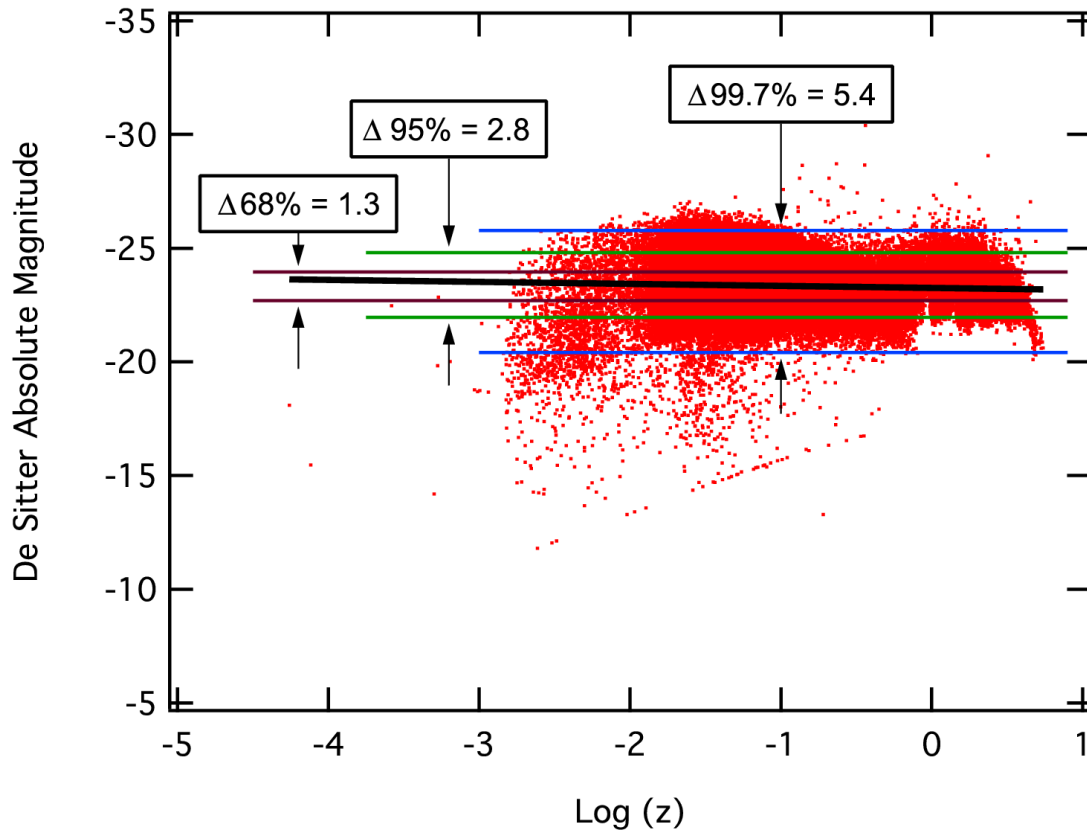


Fig. 3.— De Sitter absolute magnitude versus $\log(z)$ for SDSS galaxies and quasars. Intrinsic brightness is roughly the same at all redshifts, consistent with a quasi-static de Sitter universe.

5. Discussion

5.1. Schwarzschild-de Sitter

The de Sitter metric [equation (6)] is the minimal central mass ($M \rightarrow 0$) limiting case of the more general Schwarzschild-de Sitter metric

$$ds^2 = - \left(1 - \frac{2M}{r_1} - \frac{r_1^2}{R^2} \right)^{-1} dr_1^2 - r_1^2 [d\psi^2 + \sin^2 \psi d\theta^2] + \left(1 - \frac{2M}{r_1} - \frac{r_1^2}{R^2} \right) dt^2. \quad (22)$$

Similarly, the Schwarzschild metric

$$ds^2 = - \left(1 - \frac{2M}{r_1} \right)^{-1} dr_1^2 - r_1^2 [d\psi^2 + \sin^2 \psi d\theta^2] + \left(1 - \frac{2M}{r_1} \right) dt^2 \quad (23)$$

is the limiting case of the Schwarzschild-de Sitter metric [equation (22)] where $R \rightarrow \infty$, equivalent to a point-like central mass.

The de Sitter metric [equation (6)] can be obtained from the Schwarzschild metric [equation (23)] by recalling

$$R^2 = \frac{3}{\lambda} = \frac{3c^2}{8\pi\kappa\rho}.$$

and assuming $M = \frac{4}{3}\pi r_1^3 \rho$ (choosing units so that $\kappa = c = 1$). Others have reached similar conclusions (Baryshev 2008).

5.2. Interior Schwarzschild

The de Sitter solution has an interesting relationship to the Schwarzschild interior solution (Tolman 1934) for a perfect fluid sphere of constant density ρ ,

$$ds^2 = - \frac{dr_1^2}{1 - \frac{r_1^2}{R^2}} - r_1^2 d\theta^2 - r_1^2 \sin^2 \theta d\phi^2 + \left(A - B \sqrt{1 - \frac{r_1^2}{R^2}} \right)^2 dt^2 \quad (24)$$

where A and B are integration constants. Continuity between the interior [equation (24)] and exterior [equation (22)] Schwarzschild-de Sitter metrics at the surface of the sphere, for the limit $M \rightarrow 0$, yields $A = 0$ and $B = 1$.

The interior Schwarzschild solution puts an upper limit on the possible size of a sphere of given density. The size of the de Sitter universe is the limiting size of a perfect fluid sphere with density equal to the mean mass density of the universe. The similarity of the interior Schwarzschild metric and the de Sitter metric suggests that the de Sitter universe may be loosely construed as a giant, low-density, inside-out black hole.

5.3. Finite surface area

The surface area of the de Sitter universe is finite, even though coordinate distances such as h may be infinite. In the hyperbolic plane, the area of a maximal triangle has a finite value of π , while each of the three edges is infinitely long. Similarly, in de Sitter space, lines may be infinitely long, but surface area is finite.

5.4. Lightspeed

Assuming a de Sitter metric, there is no distinction between the three fundamental geometries with respect to the magnitude-redshift relation. However, direct lightspeed measurement is a local measurement that may bear on the reality of the hyperbolic, Euclidean, and elliptical spaces. We have found that local lightspeed from redshifted objects is normal (Miller et al. 2010), and therefore de Sitter space is presumably hyperbolic, or negatively curved.

It might be argued that any measurement of photon velocity will be local, and thereby not cosmologically relevant. However, such a measurement would be neither more nor less local than the measurement of photon redshift.

5.5. Galactic rotation

For a long time, de Sitter space was thought to be elliptical, with positive curvature and radial repulsion. However, galactic rotation curves and other dark matter phenomena suggest a radial attraction that would be present in de Sitter space with a change in sign of the radius. The sign of the radial de Sitter acceleration is mathematically somewhat arbitrary. Negatively curved de Sitter space might help explain the dark matter problem.

5.6. Supernovae

Recent work on supernovae has apparently confirmed the Hubble redshift. One might thereby assume that the de Sitter redshift could not possibly be correct. However, the supernovae data may have an alternative, self-consistent interpretation.

Current analysis assumes a time dilation factor of $1 + z$. It may be interesting to reanalyze the data without the time dilation factor to see whether the supernovae data are

consistent with a de Sitter redshift.

5.7. Black-body radiation

The discovery of the cosmic microwave background radiation (CMB) is considered a landmark test of the Big Bang model. However, the CMB may also be interpreted as a Gibbons-Hawking effect extended to the de Sitter solution (Gibbons & Hawking 1977).

6. Conclusion

Because the Hubble redshift is linear and very well-established at low redshifts, while the de Sitter redshift is quadratic at low redshifts, some may conclude that the de Sitter interpretation of the SDSS data is an aberration. However, the de Sitter redshift provides an interesting way to interpret the SDSS data and merits more study, especially given the current general interest in de Sitter theory.

Acknowledgments

Funding for the SDSS and SDSS-II has been provided by the Alfred P. Sloan Foundation, the Participating Institutions, the National Science Foundation, the U.S. Department of Energy, the National Aeronautics and Space Administration, the Japanese Monbukagakusho, the Max Planck Society, and the Higher Education Funding Council for England. The SDSS Web Site is <http://www.sdss.org/>.

The SDSS is managed by the Astrophysical Research Consortium for the Participating Institutions. The Participating Institutions are the American Museum of Natural History, Astrophysical Institute Potsdam, University of Basel, University of Cambridge, Case Western Reserve University, University of Chicago, Drexel University, Fermilab, the Institute for Advanced Study, the Japan Participation Group, Johns Hopkins University, the Joint Institute for Nuclear Astrophysics, the Kavli Institute for Particle Astrophysics and Cosmology, the Korean Scientist Group, the Chinese Academy of Sciences (LAMOST), Los Alamos National Laboratory, the Max-Planck-Institute for Astronomy (MPIA), the Max-Planck-Institute for Astrophysics (MPA), New Mexico State University, Ohio State University, University of Pittsburgh, University of Portsmouth, Princeton University, the United States Naval Observatory, and the University of Washington.

REFERENCES

- Abazajian K.N., Adelman-McCarthy J.K., Ageros M.A. et al., 2009, *ApJS*, 182, 543
- Aldrovandi R., Pereira J.G., 1996, arXiv:gr-qc/9610068v1
- Baryshev Y.V., 2008, arXiv:0810.0162v1 [gr-qc]
- Bolyai J., 1832, The absolute science of space, independent of the truth or falsity of Euclids Axiom 11 (which can never be proved a priori), *Maros-Vasarhelyini*
- Chernikov N.A., Tagirov E.A., 1968, *Ann. Inst. Henri Poincaré*, 9, 109
- de Sitter W., 1917, *MNRAS*, 78, 3
- de Sitter W., 1930, *PNAS*, 16, 474
- Dyson F.J., 1972, *Bulletin of the American Mathematical Society*, 78, 635
- Gibbons G., Hawking S.W., 1977, *Phys. Rev. D*, 15, 2738
- Gubser S.S., Klebanov I.R., Polyakov A.M., 1998, *Phys. Lett. B*, 428, 105
- Hawkins G.S., 1960, *AJ*, 65, 52
- Hilbert D., 1901, *Trans. Amer. Math Soc*, 2, 87
- Lemaître G., 1931, *MNRAS*, 91, 490
- Lobachevsky N.I., 1830, On the foundations of geometry, *Kazan Messenger* 25-28; German transl., ‘Zwei geometrische Abhandlungen’, Leipzig, 1898.
- Maldacena J., 1998, *Adv. Theor. Math. Phys.*, 2, 231
- Metsaev R.R., Tseytlin A.A., 1998, *Nucl. Phys. B*, 533, 109
- Miller J.B., Miller T.E., 1995, *Astrophysics and Space Science*, 227, 53
- Miller J.B., Miller T.E., Hoffert M.J. et al., 2010, arXiv:1012.0871 [astro-ph.CO]
- Reboul H.J., 1981, *Astron. Astrophys. Suppl. Ser.*, 45, 129
- Tolman R.C., 1934, *Relativity, Thermodynamics, and Cosmology*. University Press, Oxford
- Witten E., 1998, *Adv. Theor. Math. Phys.*, 2, 253

Zombeck M.V., 1990, Handbook of Space Astronomy and Astrophysics, 2nd Ed. Cambridge Univ. Press, Cambridge, p. 250